Chapter 6

Antibacterial Mechanism of Lysozyme coated Silver Nanoparticles against *Klebsiella pneumoniae* MGH78578

- Part of the work presented in this chapter was carried out under EMBO Short-Term Fellowship (ESTF 7654) awarded to me to work in the laboratory of Prof. Sèamus Fanning at UCD-Center for Food Safety, University College Dublin, Dublin (October-December 2018).

6.1 Introduction

The emergence of multi-drug resistant (MDR) in various pathogenic bacterial species against several most effective drugs is a massive threat to the biological society because MDR bacteria leads to cause hospital and community-acquired infection, which are tough to overcome using existing antibiotics (Nikaido, 2009). Recently, Infectious Diseases Society of America (IDSA) has scrutinized the most antibiotic-resistant bacteria and labelled as 'ESKAPE' (*Enterococcus faecium, Staphylococcus aureus, Klebsiella pneumoniae, Acinetobacter baumannii, Pseudomonas aeruginosa and Enterobacter spp.*) pathogens because of their escaping properties from host immune system and innovative patterns of resistance (Pendleton et al., 2013). Among many MDR bacterial species, *Klebsiella pneumoniae* is one of the most lethal pathogenic bacteria. It is a member of *enterobacteriacae* family, gram-negative, non-motile, rod-shaped bacteria, which is basically an opportunistic pathogenic bacterium commonly found in intestine, mouth and skin of humans. *K. pneumoniae* is mainly associated with the hospital-acquired infections (nosocomial infections) and immunocompromised person where it can cause respiratory/ urinary tract infections (UTI), pneumonia and sepsis (Podschun and Ullmann, 1998; Lee and Burgess, 2012). It is the second most UTI causing bacteria after the pathogenic strain of *Escherichia coli* (Arana et al., 2017). This bacterium is surrounded by the capsule polysaccharide (CPS), which increases it virulency by acting as a barrier between the bacteria and host's immune system thus protecting it from phagocytosis, macrophage-mediated opsonization, and desiccation (Cortés et al., 2002). Nosocomial infections are caused due to the formation of bacterial biofilm on the medical devices, which tend to be chronic because *in vivo* formed biofilms protect the bacteria from the attack of host's immune system and various antibiotics (Jagnow and Clegg, 2003; Li et al., 2014). Whole mechanism of bacterial pathogenicity is stunningly reviewed in detail by Li et al. (2014).

Apart from CPS; lipopolysaccharide, fimbriae, outer membrane proteins, efflux pumps, and many other factors are responsible for the generation of resistance in *K. pneumoniae* against various antibiotics. According to a recent U.S. based surveillance study, around 25 % of *K. pneumoniae* in long term acute hospitals were resistant to carbapenems, a commanding group of broad spectrum beta-lactam antibiotics (Han et al., 2016). Resistance to beta-lactam antibiotics, makes bacteria resistant to many antibiotics of this class, including ampicillin, carbenicillin, amoxicillin, and ceftazidime (Adamo and Margarit, 2018). Additionally, some of the *K. pneumoniae* strains are also found to be resistant to colistin and intravenous antibiotic

carbapenem (Antoniadou et al., 2007; Neuner et al., 2011). Generation of resistance in *K. pneumoniae* against major class of antibiotics is a huge threaten to the society hence, to overcome this issue there is a need of development of new antibacterial agents.

As observed in the previous chapters, silver has been found to have a tremendous antibacterial potential in its various forms, which makes it a potential candidate against MDR pathogens. In Chapter 4 and 5, we have observed the reservoir nature of lysozyme coated silver nanoparticles (L-Ag NPs), which releases the Ag^+ ions in the proximity to the bacterial cell. Hence, L-Ag NPs can be used as prospective contender against *K. pneumonia* but before the establishment of new silver based antibacterial agents, mechanism behind the antibacterial action of Ag NPs need to be resolved (Adamo and Margarit, 2018).

Antibacterial mechanism of L-Ag NPs against *K. pneumonia* MGH78578 was analysed in two steps (1) by using biochemical analysis, where the evaluation of membrane damage and reactive oxygen species (ROS) analysis was done to check the extent of damage in the bacteria under the exposure of L-Ag NPs. (2) High-throughput whole transcriptomic sequencing i.e. RNA sequencing, at different treatment times to reveal the actual molecular machinery of bacteria under the stress of L-Ag NPs. The whole transcriptomic profiling of *K. pneumonia* MGH78578 has been done as discussed in Chapter 5. Recent studies have used this technique to reveal the pathogenicity of Ag NPs against several other bacteria including *Pseudomonas aeruginosa*, *Escherichia coli*, *Campylobacter jejuni*, etc. (Sun et al., 2017; Xue et al., 2018; Singh et al., 2019).

6.2 Materials and methods

6.2.1 Materials

The details of materials used is given in Chapter 5.

6.2.2 Preparation of bacterial culture

Klebsiella pneumoniae MGH78578 (ATCC 700721) was purchased from the American Type Culture Collection, USA. Bacteria was revived from the glycerol stock and cultured in MLB broth medium (casein enzyme hydrolysate 10 g L^{-1} and yeast extract 5 g L^{-1}, pH 7.2 ± 0.2) for 12 h at 37°C under shaking (150 rpm). Considering the previous reports on precipitation of Ag^+ ions in LB media by the presence of Cl^- ions of sodium chloride salt (Chambers et al., 2013; Bhargava et al., 2018). We compared the growth of bacteria in LB media and modified LB (MLB) media (without sodium chloride), as Discussed in Chapter 3. The experiments were done in both technical & biological duplicates and the results are

represented as mean ± standard deviation (SD). The growth curve of bacteria in LB and MLB broth medium were compared.

6.2.3 Antibacterial tests

The minimum inhibitory concentration (MIC) assay was performed to determine the lowest concentration of L-Ag NPs, required to inhibit the growth of *K. pneumoniae* MGH78578 using broth microdilution method as per the standard guidelines (CLSI, 2015). Based on the MIC assay results, MBC assay was performed to find out the lowest concentration of L-Ag NPs needed to kill 99.9 % of the final inoculum (CLSI, 2015). MIC and MBC of L-Ag NPs was evaluated by following the procedure, as discussed in Chapter 3.

6.2.4 Biochemical studies

There are many known mechanisms in bacteria known to take place under the stress of silver species viz. generation of ROS, membrane damage, energy depletion, DNA damage, protein denaturation, etc. (Pareek et al., 2018). Among all different mechanisms, ROS generation and membrane damage are the two most destructive and most studied mechanisms. Hence, the preliminary antibacterial action of L-Ag NPs was analysed by measuring the ROS generation and membrane damage.

6.2.4.1 ROS generation analysis

To check the bacterial ROS generation under the exposure of L-Ag NPs, DCFH-DA assay was performed by following the protocol of Wang and Joseph (1999), with some modifications. Bacterial cells exposed to sub-MIC values of L-Ag NPs i.e. MIC_{25} [5.25 µg (Ag) mL^{-1}], MIC_{50} [10.5 µg (Ag) mL^{-1}], MIC_{75} [15.75 µg (Ag) mL^{-1}], & MIC_{100} [21.0 µg (Ag) mL^{-1}], was analysed by DCFH-DA assay, as discussed in Chapter 4.

6.2.4.2 Membrane damage analysis

The effect of silver species treatment on the bacterial cell envelope was examined by visualizing the treated bacterial cells by Scanning Electron Microscopy (SEM). Bacterial cells exposed to MIC_{75} [15.75 µg (Ag) mL^{-1}] was compared with the control bacterial cells (not exposed to L-Ag NPs), as discussed in Chapter 4.

The extent of membrane damage in the bacterial cells was further analysed in terms of lipid peroxidation measurement using malondialdehyde (MDA) assay (Buege and Aust, 1978). The membrane damage was also determined by quantifying the total sugar content using anthrone assay in the supernatant of treated bacterial cells. Estimation of MDA level and

carbohydrate in bacterial cells treated with different MIC values of L-Ag NPs, i.e. MIC_{25}, MIC_{50}, MIC_{75}, and MIC_{100} was performed as per the protocol discussed in Chapter 4.

6.2.5 Kinetics of cellular intake of silver ions by *K. pneumoniae*

The kinetics of cellular intake of silver ions from the L-Ag NPs, under as-defined conditions was determined by ICP-OES (Avio 200, PerkinElmer, USA) by following the procedure discussed in Chapter 4. Bacterial cells without L-Ag NPs treatment were taken as a control for the respective time points.

6.2.6 RNA sequencing and quantitative real-time polymerase chain reaction (qRT-PCR)

Based on the results obtained during the gene expression analysis studies in *E. coli* K12 (discussed in Chapter 4 and 5), as maximum changes were observed only at 5 and 30 min time points, these time points were selected for the transcriptomic analysis studies of *K. pneumoniae* MGH78578 exposed to MIC_{75} of L-Ag NPs. For RNA sequencing, isolation and purification of RNA was done by following the protocol discussed in Chapter 5. The RNA library preparation and subsequent sequencing were outsourced from Centre for Genomic Research, University of Liverpool, UK and in total 8 libraries were prepared as per the details given in the Table 6.1.

Table 6.1: Overview of the RNA sequencing libraries for *K. pneumoniae.*

S. no.	Name of library	Treatment time
1.	Control 5 min. (replicate 1)	5 min.
2.	Control 5 min. (replicate 2)	
3.	Test 5 min. (replicate 1)	
4.	Test 5 min. (replicate 2)	
5.	Control 30 min. (replicate 1)	30 min.
6.	Control 30 min. (replicate 2)	
7.	Test 30 min. (replicate 1)	
8.	Test 30 min. (replicate 2)	

Preparation of RNA libraries and raw sequencing data were processed as discussed in the Chapter 5. For the validation of RNA seq. data, quantitative RT-PCR was performed. RNA isolated from the above-mentioned samples were converted to cDNA by using High-capacity RNA to cDNA kit (Thermo fisher, Dublin, Ireland), as per the manufacturer's instruction.

Primers of genes of interest were designed with 6-FAM/ZEN/IBFQ double-quenched probes and synthesized from Integrated DNA Technologies (IDT, Leuven, Belgium) (Table 6.2).

Table 6.2: Details of gene specific primers used for qRT-PCR.

S. No.	Genes	Sequence	Amplicon size
1.	***ompC***	FWD: TGGTCGTTGATCTGGGTTTC	99
		REV: AATTGACGGTCTGCACTACTT	
		PRB: /56-FAM/CATGCGTGT/Zen/AGGCGT GAAAGGC/3IABkFQ/	
2.	***ramA***	FWD: TTCCGCTCAGGTGATTGATAC	104
		REV: TTGCAGATGCCATTTCGAATAC	
		PRB: /56-FAM/TAACCTGCA/Zen/TCAACCGCT GCGTAT/3IABkFQ/	
3.	***rfaH***	FWD: TGCGTTTACCGCGAATGA	106
		REV: AAACGTGGGCAGCTACAA	
		PRB: /56-FAM/ACTGACGTT/Zen/CCAGATGTT CCTGGG/3IABkFQ/	
4.	***soxS***	FWD: GCATCACGGTACGGAACAT	112
		REV: GATGAACATATCGATCAACCACTTAAC	
		PRB: /56-FAM/TCGAGTATC/Zen/CTGACTTTCT GGCGACT/3IABkFQ/	
5.	***rho***	FWD: CTCAGGAAGAGCTGCAGAAA	108
		REV: CTTGGTCATTGCCAGCTTATTG	
		PRB: /56-FAM/CGATGGGTG/Zen/AGATTGA TGCGATGGA/3IABkFQ/	

This cDNA was used as a template and analysis was done by the addition of PrimeTime Gene Expression Master Mix. RT-PCR was performed in an Eppendorf Mastercycler realplex ep gradient S (Eppendorf, Arlington, United Kingdom), as per the manufacturer's instruction. This analysis was done two biological replicates each with three technical replicates. The fold change in the expression of gene was determined by the method of Livek and Schmittgen (2001), i.e. $2^{-\Delta\Delta Ct}$ method by using *rho* as a housekeeping gene.

6.2.7 Statistical analysis

The results for the biochemical assay were analysed using unpaired Student t-test as appropriate for the data set. The qRT-PCR measurements data were statistically analysed using Prism software (Version 8.0; GraphPad Software Inc.) (Motulsky, 1999). The symbol 'ns' used in the graphs shall be interpreted as statistically non-significant at $P > 0.05$. The asterisk symbols in the graphs can be interpreted as: * $P \leq 0.05$, ** $P \leq 0.01$, and *** $P \leq 0.001$.

6.2.8 Transmission electron microscopy

Transmission Electron Microscopy (TEM) measurements were carried out to determine the morphology of the bacteria after the L-Ag NP treatment and the bacterial cells exposed to MIC_{75} concentration of L-Ag NPs for 30 min. was compared with the cells not exposed to L-Ag NPs (control). The preparation of samples for the TEM analysis was done by following the procedure discussed in Chapter 5.

6.3 Results and Discussion

6.3.1 Bacterial growth kinetics

K. pneumoniae MGH78578 is a clinical isolate, originally isolated from the 66 years old ICU patient in 1994. This strain was chosen because of its multidrug resistance against various antibiotics including ampicillin, ticarcillin, trimethoprim-sulfamethoxazole, gentamicin, etc. (Ogawa et al., 2005; Anes et al., 2019) The main advantage behind the selection of this strain was the availability of whole genome sequence (Reference Sequence NC_009648.1).

LB broth medium is a complex medium used for the cultivation of *K. pneumoniae* and It is comprising of casein enzyme hydrolysate, yeast extract, and sodium chloride with a quantity of 10, 5 and 5 g L^{-1}, respectively (Deininger, 1990; Favre-Bonte et al., 1999). As discussed in the Chapter 3, biological medium components can make significant difference in the antibacterial activity of silver species. In LB media, presence of Cl^- ion of sodium chloride salt, which maintain tonicity of media, has been reported to cause precipitation of Ag^+ ions in the form of silver chloride (McQuillan et al., 2012; Chambers et al., 2013). This may result in the reduced availability of free Ag^+ ions and thus, reduction in the bactericidal activity. In order to overcome the precipitation issue, we have compared the growth of *K. pneumoniae* MGH78578 in LB media and MLB media lacking sodium chloride, by following the procedure discussed in Chapter 3 (Bhargava et al., 2018).

The obtained growth curve (Figure 6.1) showed the absence of lag phase in case of LB media as the young growing bacterial cells were used as inoculum and transferred to fresh LB media with same compositions. Interestingly, no lag phase was observed in case of MLB media (lacking NaCl) as well. In both media types, the duration of log phase was found to be 8 h. A non-significant difference was observed in the overall growth pattern of *K. pneumoniae* MGH78578 in both media types. Based on these results, MLB media was chosen for the further antibacterial studies.

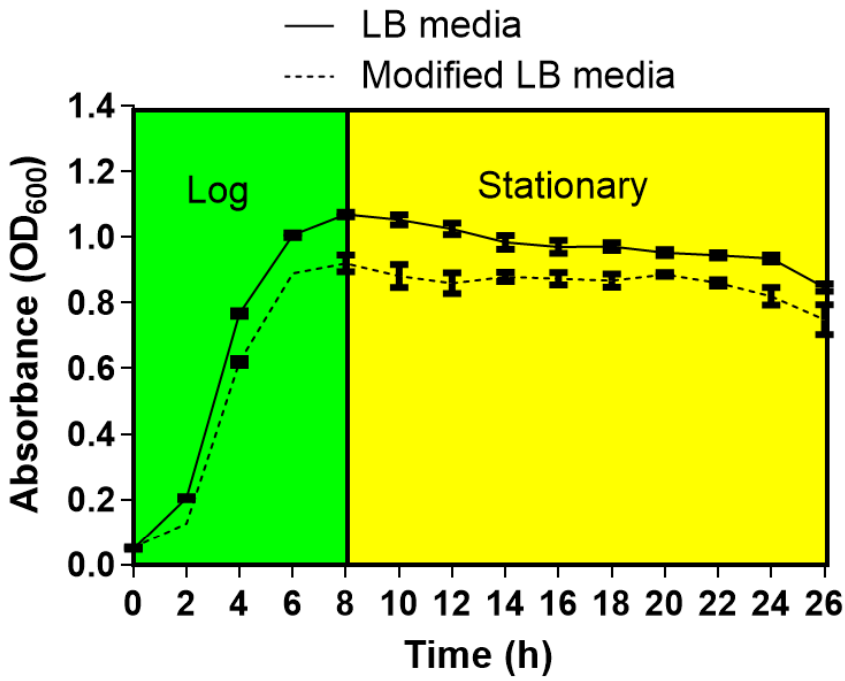

Figure 6.1: Growth curve analysis of *K. pneumoniae* in LB and MLB media. Vertical bar represents SD.

6.3.2 Antibacterial activity

For the analysis of antibacterial activity, ~3×10^7 CFU mL^{-1} of freshly grown *K. pneumoniae* culture was exposed to different concentrations of L-Ag NPs and observed for growth till the completion of log phase. Antibacterial activity of synthesized Ag NPs was analysed by MIC and MBC assay. The MIC is the lowest concentration of antimicrobial agent that completely inhibit the growth of microorganisms (CLSI, 2015) and the MIC of L-Ag NPs was found to be 21 µg (Ag) mL^{-1} (Figure 6.2).

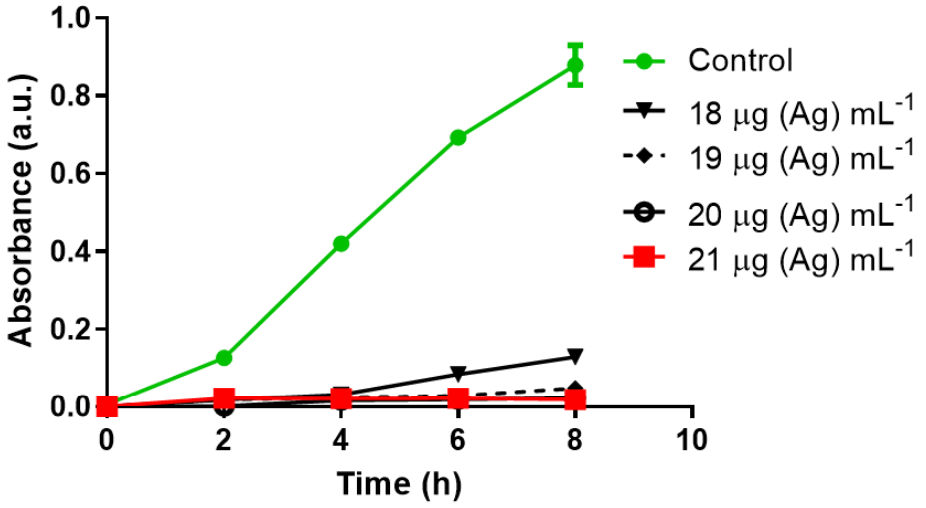

Figure 6.2: MIC evaluation of L-Ag NPs against *K. pneumoniae*. Vertical bar represents SD.

MBC assay was performed to find out the lowest concentration of silver species (silver ions/ Ag NPs) needed to kill 99.9 % of the final inoculum after incubation for 24 h under standardized conditions (CLSI, 2015). The lowest concentration of L-Ag NPs causing bactericidal effect was selected based on the absence of visual bacterial growth on agar plates and reported as MBC. Representative images of MBC analysis for verifying concentrations of L-Ag NPs have been shown in Figure 6.3, which confirmed the MBC of L-Ag NPs to be 45 µg (Ag) mL^{-1}.

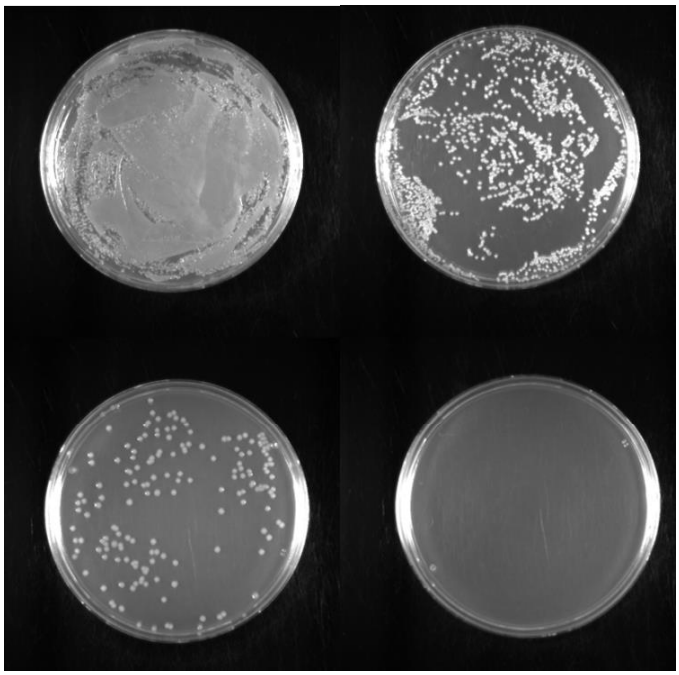

Figure 6.3: MBC analysis for verifying concentrations (A) 0 (Control), (B) 43, (C) 44, and (D) 45 µg (Ag) mL^{-1} of silver ions against *K. pneumoniae*.

The MBC/MIC ratios were calculated to determine the presence or absence of tolerance to silver species. A bacterium is known to be tolerant to any antibacterial agent, when the MBC/MIC ratio value is found to be ≥ 32 (Sader et al., 2006; Traczewski et al., 2009; Gonzalez et al., 2013). The MBC/MIC ratio for L-Ag NPs was found to be 2.14, which means no tolerance was exhibited, it suggested that L-Ag NPs can be used as an alternative to standard therapy for bacterial infections.

6.3.3 Biochemical assays

Growth of bacteria can be controlled by targeting and disturbing the oxidative phosphorylation of respiratory chain, membrane integrity, enzyme activity, etc. of some of the pivotal metabolic pathways (Jain et al., 2015; Yun'an Qing et al., 2018). Among all these pathways, increase in the generation of ROS and damage to the bacterial cell membrane cause maximum harm to the bacterial cells (Park et al., 2009). Based on these facts, we inclined to select and analyse these two major pathways in the present study.

As discussed in Chapter 4, to investigate the generation of free radicals in the bacterial cells exposed to L-Ag NPs, DCFH-DA assay was performed, which measures the signal intensity of fluorescent product namely dichloro fluorescein (DCF) formed due to oxidation of non-fluorescent compound DCFH in presence of intracellular ROS (Rastogi et al., 2010). Figure 6.4 A shows the extent of free radicals generated from the bacterial cells treated with various concentrations of L-Ag NPs by considering untreated bacterial cells as control. The induction of ROS was found to be directly proportional to the concentration of treatment. Bacteria treated with MIC_{100} of L-Ag NPs has produced ~80 times higher ROS than their respective controls.

SEM measurements were carried out to determine the morphology of bacterial cells after treatment with L-Ag NPs. SEM micrographs of representative bacterial cells show very less damage in the bacterial cell membrane in comparison to the control (Figure 6.4 B and C, and)

A concentration-dependent increase in the level of lipid peroxidation was observed for L-Ag NPs treated cells in comparison to control, which suggests the damage/ leakage in the bacterial membrane (Figure 6.4 D). Recently, our research group has worked on the chemical synthesis of Ag NPs and analysed their antibacterial potential by various methods including ROS and MDA analysis, where concentration dependent increase was observed in both ROS generation and lipid peroxidation (Bhargava et al., 2018).

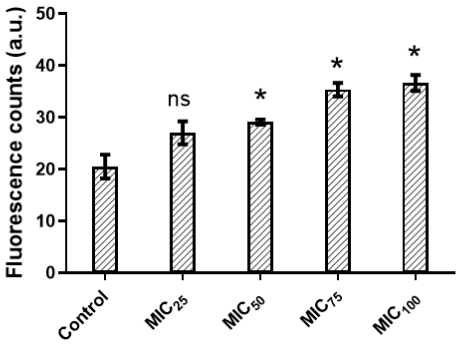

(A)

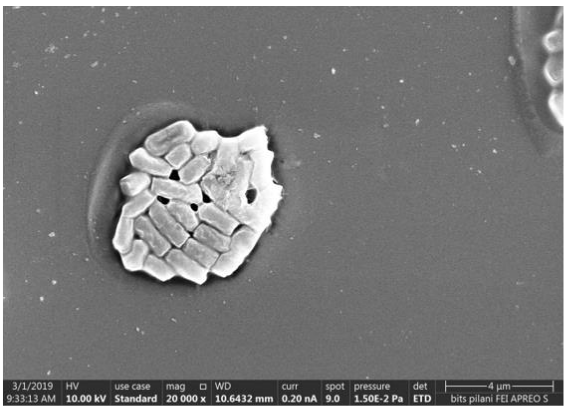

(B)

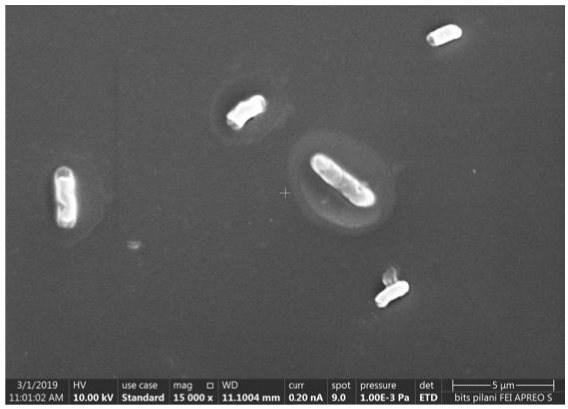

(C)

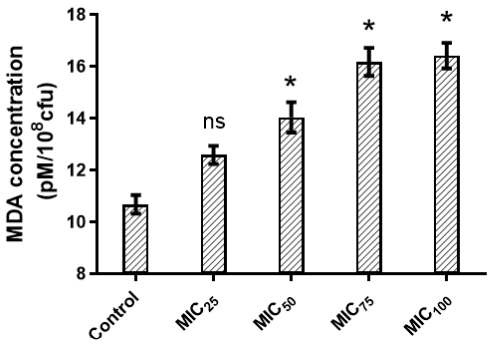

(D)

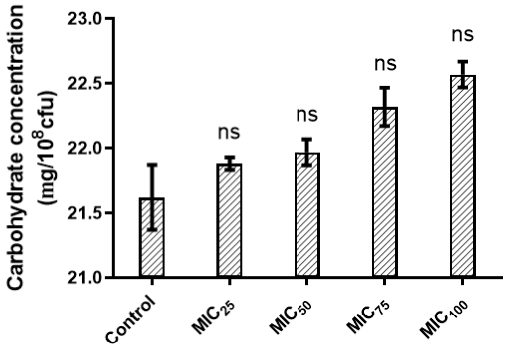

(E)

Figure 6.4: Biochemical analysis of *K. pneumoniae* exposed to MIC_{75} of L-Ag NPs in comparison to control (A) ROS generation by DCFH-DA assay; SEM micrograph showing the membrane damage in the bacteria treated with (B) Untreated/ control, (C) MIC_{75} of L-Ag NPs; (D) MDA assay, and (E) Anthrone assay. Vertical bars represent SD.

In addition, the carbohydrate released from the bacterial cells was measured to find out the level of membrane damage upon L-Ag NPs exposure. Unlike ROS generation and MDA assay results, a non-significant increase was observed for the carbohydrates released outside the bacterial cells (Figure 6.4 E). It is well evident that damage to bacterial membrane can

results in release of intracellular compounds (Singh et al., 2016; Miller and Salama, 2018). The obtained results suggested a less significant increase in the lipid peroxidation of bacterial membrane which eventually resulted in the release of intracellular carbohydrate (non-significant) from the bacterial cell.

6.3.4 Kinetics of cellular uptake of silver by *K. pneumoniae*

To find out the concentration of silver ions which entered inside the *K. pneumoniae*, the cells treated with the MIC_{75} of L-Ag NPs for 5, 30 and 60 min. were separately subjected to the acid digestion. It resulted in release of silver ions from the bacterial cytoplasm, which was measured by the ICP-OES analysis (McQuillan et al., 2012; Jain et al., 2015). Uptake of less silver ions in bacterial cells exposed to L-Ag NPs showed the controlled and sustained release of silver ions, which makes it better antibacterial agent (Figure 6.5).

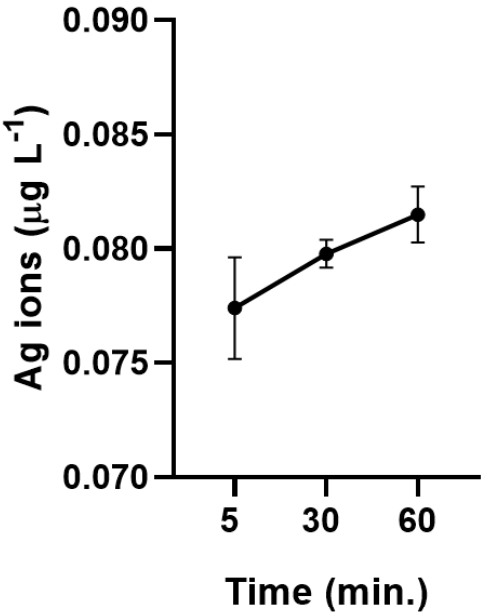

Figure 6.5: Concentration of silver ions in *K. pneumoniae* cells exposed to MIC_{75} of L-Ag NPs. Vertical bar represents SD.

6.3.5 RNA sequencing analysis

To get the idea about the mechanistic aspects behind the action of L-Ag NPs, whole transcriptomic analysis was done by using high throughput RNA sequencing analysis. *K. pneumoniae* MGH78578 was treated with MIC_{75} of L-Ag NPs for 5 and 30 min time points. Time of treatment was selected on the basis of replication time of bacteria. The 5 min. time point was used to identify the early transcriptional signals following L-Ag NPs exposure,

whereas the 30 min. time point was used to identify the adaptive responses of *K. pneumoniae* cells. Bacteria without any treatment was taken as a control for their respective time points. RNAseq raw data provided about 336 million reads across all the 8 libraries with an average of 42 million reads per library which is a significant number for the transcriptomic analysis in *K, pneumoniae* (Haas et al., 2012; Anes et al., 2019).

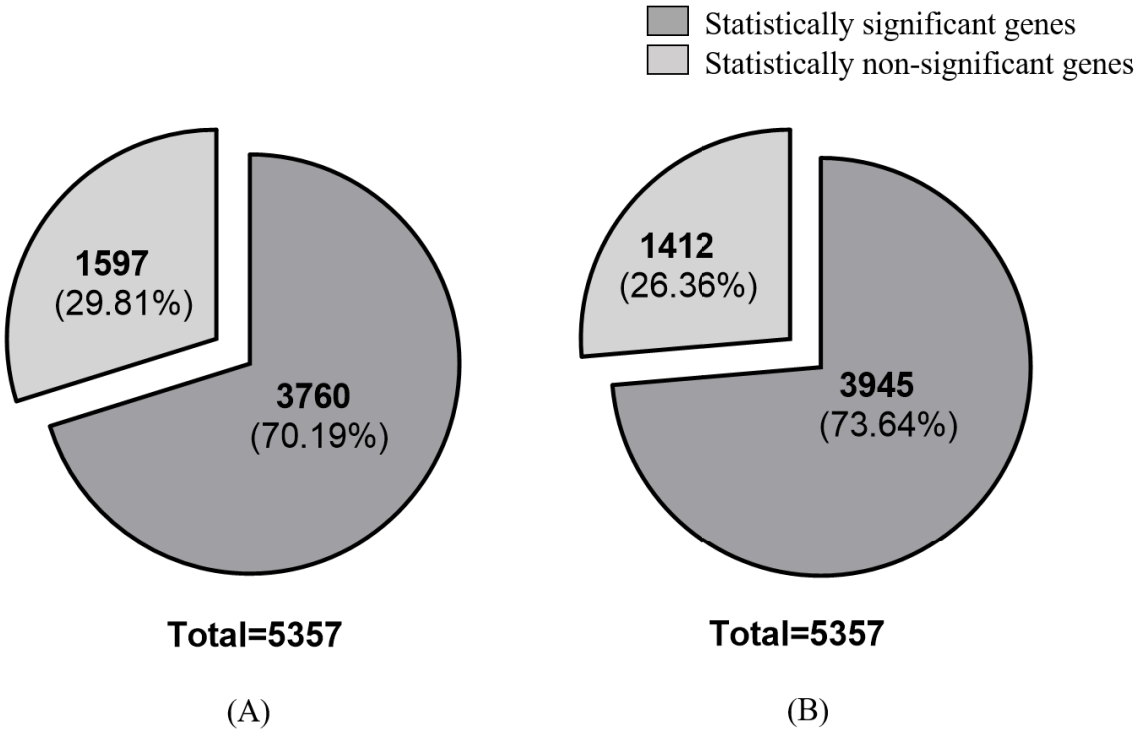

Figure 6.6: Overview of statistically significant and non-significantly expressed (NSE) genes at (A) 5 min. and (B) 30 min., post L-Ag NPs exposure (FDR, $p \leq 0.05$).

Differential expression of all the genes of *K. pneumoniae* was identified using *VOOM* function in the *limma* package (Ritchie et al., 2015). Differential gene expression was obtained for total 5357 genes upon exposure of *K. pneumoniae* to L-Ag NPs for 5 and 30 min. time points. Among all the differentially expressed genes, statistically significant genes were selected by setting FDR value at $p \leq 0.05$ (adjacent p value) (Anes et al., 2019). Among all 5357 genes, 3760 and 3945 genes were found to be statistically significant in case of 5 min. and 30 min., respectively (Figure 6.6). Genes with a $\log_2$ fold change value of ≥ 1.0 and ≤ -1.0 were considered to be up-regulated and down regulated, respectively (Dash et al., 2018; Anes et al., 2019). On this basis, 1008 genes were found to be upregulated, 1063 genes were down regulated, and 1689 genes remained neutral at 5 min. post L-Ag NPs exposure. However, at 30 min., treatment, 1205 genes were found to be upregulated, 1246 genes got downregulated, and 1494 genes remained neutral (Figure 6.7).

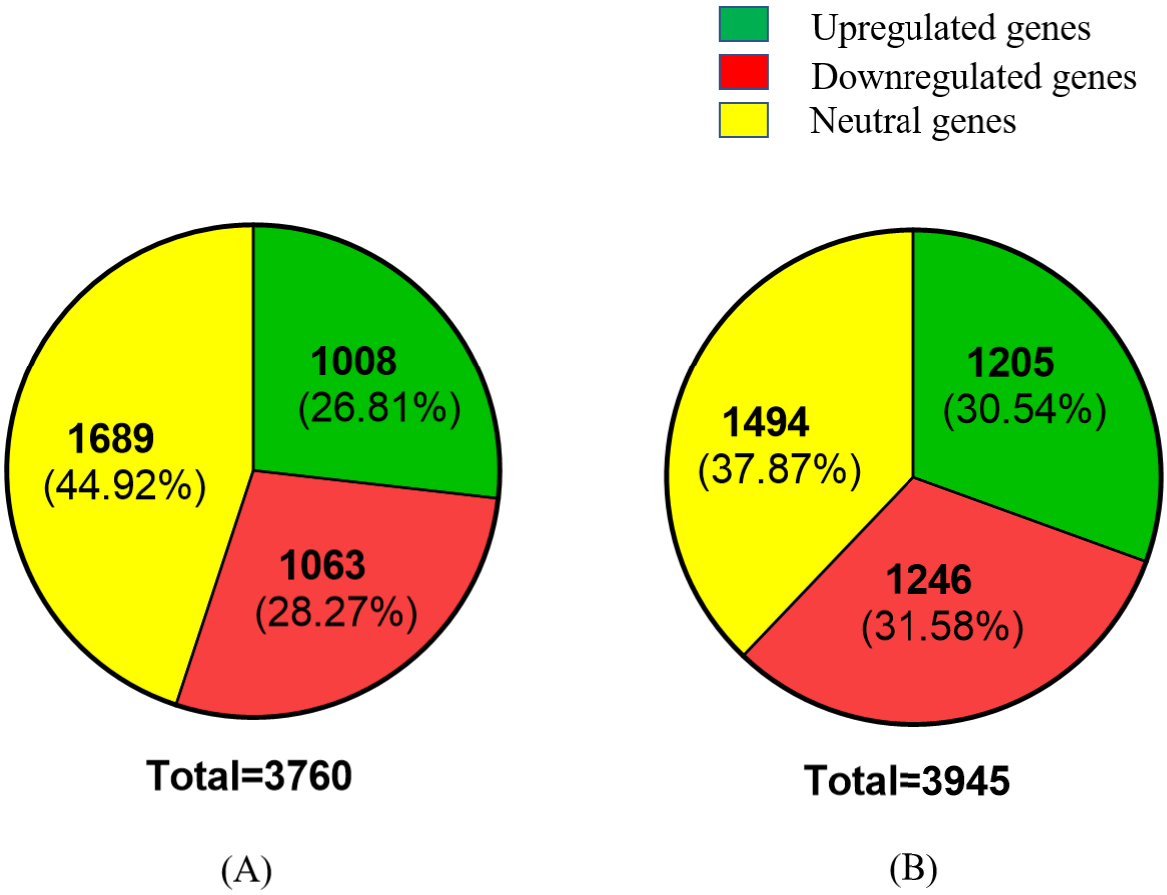

Figure 6.7: Overview of significantly expressed genes at (A) 5 min., and (B) 30 min. post L-Ag NPs exposure.

Among all the up-regulated genes at 5 and 30 min. post L-Ag NPs exposure, 705 genes were found to be commonly upregulated whereas, 303 and 500 genes were specifically up-regulated in 5 min. and 30 min. treatment, respectively. In case of down-regulated genes, 810 genes were found to be commonly down-regulated at both time points whereas, 253 and 436 genes were specifically down-regulated in 5 min. and 30 min. treatment. 807 genes were commonly found in neutral category (Figure 6.8).

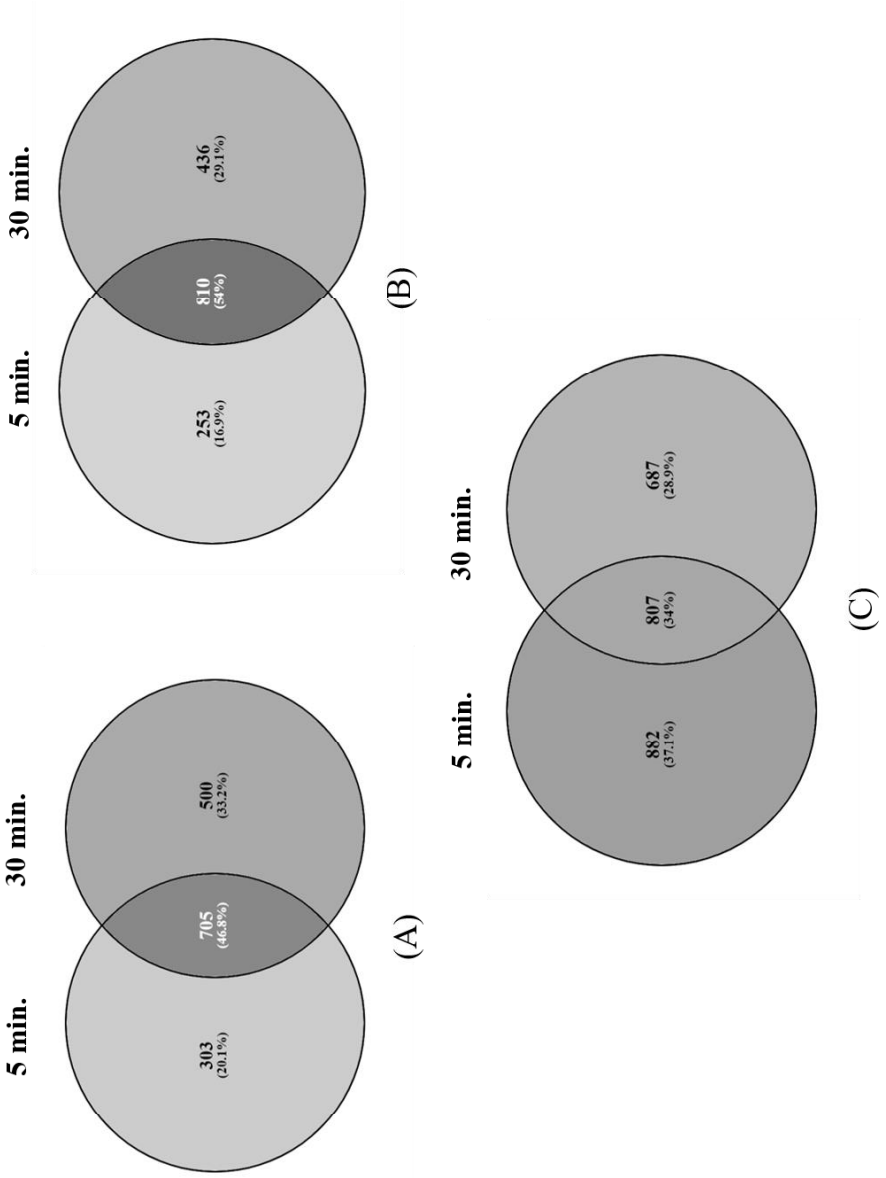

Figure 6.8: Venn diagram showing overlapping sets of differentially (A) up-regulated, (B) down-regulated and (C) neutral genes at 5 and 30 min. treatment post L-Ag NPs exposure

In the present study, differential expression pattern of genes probably involved in the antibacterial activity of Ag NPs was analysed. *K. pneumoniae* MGH78578 is a non-motile and non-flagellar bacterium, which allows the direct contact of bacterial cell with L-Ag NPs (Ashurst and Dawson, 2019).

Bacterial envelope of gram negative bacteria is made up of three different layers viz. outer membrane lipopolysaccharide (LPS), peptidoglycan cell wall, and plasma membrane. The Ag^+ ions released from the L-Ag NPs first encounter the outer membrane of *Klebsiella pneumoniae*, through which they can enter into the bacterial cell. As discussed in Chapter 4,

for the entry of silver ions into the bacteria, there are two likely pathways by that ions can enter bacterial cell viz. (1) by damaging the bacterial membrane and (2) by porin proteins. Hence, we have considered LPS layer for the differential gene expression study (outermost layer of bacterial membrane) (May and Grabowicz, 2018). In the present study, the LPS synthesis genes were investigated to check the membrane damage which eventually allow the entry of Ag^{+} ions into the bacterial cells. Differential expression pattern of genes related to the LPS synthesis did not show any sign of membrane damage as most of the genes were found to be neutral, which suggest that silver ions could not damage the bacterial outer membrane (Table 6.3). In case of membrane damage, downregulation of LPS synthesis genes would have been observed due to the activation of alternate sigma factor to direct RNA polymerase towards their specific promotors, hence inducing a set of genes or regulon(s) to combat the stress response (Regué et al., 2001; Kazmierczak et al., 2005).

Table 6.3: Differential expression profile of lipopolysaccharide biosynthesis regulating genes under the stress of L-Ag NPs.

Gene ID	Gene name	Log_2 fold change		Protein annotation
		5 min.	30 min.	
KPN_RS06850	*yciM*	0.845786	0.562136	Lipopolysaccharide assembly protein LapB
KPN_RS21400	*waaL*	-0.613297	-1.14581	O-antigen polymerase
KPN_RS21385	*waaF*	0.636781	0.51601	ADP-heptose--LPS heptosyltransferase
KPN_RS18515	*rfaE*	-0.606778	-0.23622	Bifunctional heptose 7-phosphate kinase/heptose 1-phosphate adenyltransferase
KPN_RS21435	*waaA*	-0.372266	-0.44815	3-deoxy-D-manno-octulosonic acid transferase
KPN_RS21440	*waaE*	-0.391755	-0.27379	LPS biosynthesis protein
KPN_RS05710	*htrB*	0.574996	0.914438	Lipid A biosynthesis lauroyl acyltransferase

To check another pathway for the entry of silver ions into bacterial cell, the genes related to the synthesis of porin proteins were analysed. Upon the differential expression analysis, it has been observed that the gene expression of *phoE* gene got up-regulated to 3.01 and 5.37 log_2 fold for 5 min. and 30 min. time points, respectively (Table 6.4). PhoE is an outer membrane porin protein that allows the entry of inorganic phosphate and some negatively charged solutes (Kaczmarek et al., 2006). Other than PhoE, none of the porin protein was found to be involved in the transport of silver ions. Since these porin proteins have a channel of angstrom size, NPs cannot pass through, but ions can easily pass, which suggests the action of L-Ag NPs is not acquired by the nano form, but the silver ions released constantly from its nano form. Entry of silver ions through porin proteins can be linked with the entry of antibiotics into the cell by diffusive porin proteins (Ghai and Ghai, 2018).

Table 6.4: Differential expression profile of porin protein biosynthesis regulating genes under the stress of L-Ag NPs.

Gene ID	Gene name	Log_2 fold change		Protein annotation
		5 min.	30 min.	
KPN_RS01515	*phoE*	3.01418312	5.374805	Phosphoporin PhoE
KPN_RS04550	*ompX*	0.7160045	1.794181	Outer membrane protein X
KPN_RS07750	*ompN*	0.93424393	-1.08474	Phosphoporin PhoE
KPN_RS14160	*ompC*	0.74757967	-1.01107	Phosphoporin PhoE
KPN_RS13100	KPN_02430	NSE	1.248405	Phosphoporin PhoE
KPN_RS05140	*ompF*	0.95253847	NSE	Hypothetical protein
KPN_RS05295	*ompA*	0.24045598	NSE	Porin OmpA
KPN_RS03770	*ybfM*	-2.3669638	-2.44766	Chitoporin
KPN_RS02750	KPN_00515	NSE	-1.55807	Sucrose porin
KPN_RS02300	KPN_00433	NSE	-0.99435	Maltoporin
KPN_RS04895	*aqpZ*	NSE	-1.96663	Aquaporin
KPN_RS21630	*glpF*	-1.7970857	-1.79203	Aquaporin
KPN_RS23815	*lamB*	0.88951564	NSE	Maltoporin
KPN_RS17520	*yjhA*	-0.7701898	NSE	Porin
KPN_RS25745	KPN_04773	0.3686468	-1.21592	Porin
KPN_RS00900	*fhuA*	0.16256757	1.572208	Ferrichrome porin FhuA

As discussed in Chapter 4, once silver ions get inside the bacterial cell, there is an increase in the generation of intracellular reactive oxygen species (ROS). Increase in the ROS inside the cell can be directly correlated with the rise in the level of free radical quenching enzymes like superoxide dismutase (SOD) (regulated by *sodA*, *sodB* and *sodC*), catalase (regulated by *katE* and *KatG*), and peroxidase (regulated by *AhpC* and *gst*) which specifically quench superoxide anions (O_2^-) and peroxides such as hydrogen peroxide (H_2O_2), respectively (Niederhoffer et al., 1990; Farr and Kogoma, 1991). In order to find out which kind of ROS has been generated, different ROS generating mechanism were analysed by studying differential expression of ROS regulating genes under the stress of L-Ag NPs. The obtained results showed an up-regulation in the expression of *sodA* gene to 2.40 and 2.98 $\log_2$ fold for 5 and 30 min. time point, respectively. Up-regulation in the gene expression of *sodA* gene suggests the increase in generation of superoxide radicles. Increase in ROS was also contributed by the generation of H_2O_2 radicals, which was proven by the up-regulation of *gst* gene to 1.19 and 3.38 $\log_2$ fold for 5 and 30 min. post L-Ag NPs exposure, respectively (Huang et al., 2013) (Table 6.5). Other than *sodA* and *gst* genes, most of genes showed either neutral or statistically non-significant expression (NSE).

Table 6.5: Differential expression profile of ROS regulating genes under the stress of L-Ag NPs.

Gene ID	Gene name	$\log_2$ fold change		Protein annotation
		5 min.	30 min.	
KPN_RS22735	*sodA*	2.4078445	2.9863563	Superoxide dismutase
KPN_RS10720	*sodB*	0.3987772	-1.6512566	Superoxide dismutase
KPN_RS10670	*sodC*	0.3298202	0.5593199	Superoxide dismutase
KPN_RS10610	*gst*	1.1927878	3.2887397	Glutathione S-transferase

To combat the increased intracellular ROS, bacterial cell have two defence machineries viz. oxyR system and soxRS system where, OxyR system is known to be the global regulator of peroxide stress and SoxRS system is involved in the control of superoxide stress (Zheng et al., 1998; Seo et al., 2015). Increase in the intracellular ROS induces the oxidation of oxyR protein and the oxidized oxyR further activate the other detoxifying processes like heme biosynthesis, reductant supply, thiol-disulfide isomerization, etc. (Dubbs and Mongkolsuk, 2012). In case of SoxRS system, oxidative stress leads to oxidize the soxR protein (constitutively expressed), which in turn activated the *soxS* and it acts as a activator for bacterial

defence mechanism by stimulating the action of various efflux pumps and redox counter mechanisms (Seo et al., 2015). Differential analysis of genes related to OxyR and SoxRS systems showed that expression of *soxS* was maximum (8.35 log_2 fold up-regulation) among all the genes at 5 min. time point, which reduced to 6.46 log_2 fold up-regulation at 30 min. time point. The obtained results confirmed that SoxRS machinery is mainly responsible for the regulation of oxidative stress upon exposure to L-Ag NPs. Differential expression pattern of *soxS* showed that bacteria could sense the stress conditions silver ions at the initial time point (5 min.) and activated its defence mechanism upon the adaptation to stress (30 min.), which prevented further up-regulation in the expression of *soxS* gene. As a response of *soxS* activation, redox neutralization process gets started which is related to the overexpression of *fpr* [ferredoxin-NADP(+) reductase] to 4.51 fold at 5 min. which further decreases to 3.20 fold at 30 min. treatment (Krapp et al., 2002). This decrease in the expression of *soxS* and *fpr* can be correlated with the increase in the upregulation of *gst*, which has quenched the superoxide anion radicles (Huang et al., 2013) (Table 6.6).

Table 6.6: Differential expression profile of genes related to bacterial defence under the stress of L-Ag NPs.

Gene ID	Gene name	Log_2 fold change		Protein annotation
		5 min.	30 min.	
KPN_RS22905	*oxyR*	2.347637	2.505207	DNA-binding transcriptional regulator OxyR
KPN_RS24030	*soxR*	-0.96823	0.643518	DNA-binding transcriptional dual regulator SoxR
KPN_RS24025	*soxS*	8.350219	6.469194	AraC family transcriptional regulator
KPN_RS21590	*fpr*	4.514915	3.202294	Ferredoxin--NADP(+) reductase

Now a question arises that whether these changes in the bacterial functioning under the stress of L-Ag NPs affect the DNA/ protein processing or not? To check these aspects, we have analysed differential expression of genes related to the DNA and protein repair machinery. In this regard, SOS response machinery and protein chaperons were analysed, as discussed in Chapter 4. In general, oxidative stress causes damage in the bacterial DNA depending on the type, concentration and exposure time of antibacterial agents (Gurbanov et al., 2018).

In brief, SOS response process has two main proteins which governs the whole repair process viz. LexA (repressor protein) and RecA (an inducer protein). In presence of DNA damage, RecA protein acts on the LexA protein which is bound to SOS box (regulon of ~50 genes) to prevent the activation of SOS repair machinery (Žgur-Bertok, 2013). Differential expression analysis showed that DNA processing was not much affected upon exposure of bacterial cells to MIC_{75} concentration of L- Ag NPs, as no significant change in the expression pattern of genes related to the DNA repair machinery were observed (Table 6.7).

Table 6.7: Differential expression profile of genes related to DNA repair mechanism under the stress of L-Ag NPs.

Gene ID	Gene name	Log_2 fold change		Protein annotation
		5 min.	30 min.	
KPN_RS03795	*ybfE*	-2.55497	-2.01121	LexA regulated protein
KPN_RS16255	*recA*	1.021644	1.121854	DNA recombination/repair protein RecA
KPN_RS13000	*uvrC*	0.385437	NSE	Excinuclease ABC subunit C
KPN_RS13005	*uvrY*	0.292378	NSE	DNA-binding response regulator
KPN_RS23845	*lexA*	NSE	0.511411	DNA-binding transcriptional repressor LexA
KPN_RS04345	*uvrB*	NSE	0.589033	Excinuclease ABC subunit B

Similarly, to check the effect of silver ions on intracellular proteins, molecular chaperones/ chaperonins were taken into consideration. Molecular chaperones/ chaperonins basically interact with the partially folded or unfolded proteins and facilitate the actual folding of proteins (Rigel and Silhavy, 2012). Since bacterial cytoplasm has thousands of proteins, the expression pattern of DNA damage repair machinery cannot be correlated with the protein repair machinery. Expression of *dnaK* showed the 4.98 and 2.5 log_2 fold up-regulation at 5 min. and 30 min., respectively (Table 6.8). This decrease in the expression can be correlated to the activation of bacterial defence system where some of the proteins got back into their native folding state. Likewise, high up-regulation was also found in the gene expression pattern of many other genes like *htpG*, *ibpA*, dnaJ, etc. at 5 min. and 30 min. post L-Ag NPs exposure. Increase in the expression of protein chaperons can be correlated with activation of alternative sigma factor (Kazmierczak et al., 2005). This leads to the up-regulation of molecular chaperon

in order to prevent protein misfolding & aggregation, and help the bacterial cell to survive under the stress of L-Ag NPs (Rhodius et al., 2005; Rollauer et al., 2015).

Table 6.8. Differential expression profile of genes related to protein repair mechanism under the stress of L-Ag NPs.

GENE ID	Gene name	Log_2 fold change		Protein annotation
		5 min.	30 min.	
KPN_RS00070	*dnaK*	4.946306	2.654613	Molecular chaperone DnaK
KPN_RS22070	*ibpA*	6.767532	6.494519	Heat-shock protein IbpA
KPN_RS02415	*htpG*	5.027014	3.952839	Molecular chaperone HtpG
KPN_RS00075	*dnaJ*	2.716558	1.322638	Molecular chaperone DnaJ
KPN_pKPN3p05898	KPN_pKPN3p05898	2.457153	4.423798	Molecular chaperone (small heat shock protein)
KPN_RS24450	*groEL*	4.588748	2.808397	Chaperonin GroEL
KPN_RS15345	*hscB*	-0.29056	NSE	Co-chaperone protein HscB

The observed changes occurred in the protein chaperones motivated us to test that how does bacteria keep up its cellular homeostasis under the stress of L-Ag NPs? As discussed in Chapter 4, *E. coli* (gram-negative modal organism) maintains its homeostasis by iron-sulfur cluster (ISC) pathway which has two major protein viz. IscU and IscS, transcribed by *iscU* and *iscS*, respectively (Roche et al., 2013). Differential expression analysis of these genes along with some other related genes, did not show any significant change which suggests the active homeostasis of bacteria. However, change in the intracellular protein folding leads to disturb homeostasis at some extent. In this stress condition, homeostasis is maintained by Suf system, which is a complex of six proteins, i.e. SufA, SufB, SufC, SufD, SufS, and SufE (Fontecave et al., 2005). Differential expression profile of Suf machinery genes was found to be directly proportional to the time of treatment, as increase in the time of treatment increases the up-regulation in gene expression, which suggests that homeostasis has been disturbed due to the action of L-Ag NPs, i.e. interruption in the protein folding process (Table 6.9).

Table 6.9: Differential expression profile of genes related to bacterial homeostasis mechanism under the stress of L-Ag NPs.

Gene ID	Gene name	Log_2 fold change		Protein annotation
		5 min.	30 min.	
KPN_RS15355	*iscU*	0.386436	0.716377	Fe-S cluster scaffold-like protein
KPN_RS15365	*iscR*	0.395085	1.030988	Fe-S cluster assembly transcriptional regulator IscR
KPN_RS15360	*iscS*	0.402848	0.518496	IscS subfamily cysteine desulfurase
KPN_RS15350	*iscA*	0.334051	0.739186	Iron-binding protein
KPN_RS15335	*fdx*	-0.3527	-0.28207	Ferredoxin%2C 2Fe-2S type%2C ISC system
KPN_RS15330	*yfhJ*	-0.30285	NSE	Fe-S assembly protein IscX
KPN_RS11535	*sufB*	2.906543	6.664506	Fe-S cluster scaffold complex subunit SufB
KPN_RS11530	*sufC*	2.264624	5.994093	Fe-S cluster scaffold complex subunit SufC
KPN_RS11525	*sufD*	1.533682	5.850701	FeS cluster assembly protein SufD
KPN_RS11520	*sufS*	1.002614	NSE	L-cysteine desulfurase
KPN_RS11515	*sufE*	4.291024	5.656799	Cysteine desulfuration protein SufE

In order to maintain homeostasis in *K. pneumoniae* through Suf system, exposure of L-Ag NPs also stimulated the expression of cysteine biosynthesis genes. Cysteine is the most commonly found amino acid in the functional site of proteins and is susceptible to oxidation due to the occurrence of ROS, which is essentially required for the construction of Iron-Sulfer cluster complex (Poole, 2015). As discussed in Chapter 5, cysteine biosynthesis is required for many other biological processes and the synthesis of cysteine can be achieved through three different precursor materials viz. sulfate, taurine and alkenosulfonates, which synthesize sulphite with the help of *cys*, *tauABCD* and *ssuABC* gene clusters, respectively (van der Ploeg et al., 2001). Differential analysis of these gene cluster showed that most of the cysteine is synthesized by utilizing sulfate as a starting material whereas, taurine is utilized second after sulfate followed by alkenosulfonates in case of L-Ag NPs treated *K. pneumoniae* MGH78578. Differential expression analysis showed that 5 min. post L-Ag NPs exposure resulted in the maximum up-regulation of *cys* and *tauABCD* gene clusters. At 30 min. time point, a decrease

was observed in the up-regulation of all the gene cluster, whereas, non-significant expression was observed for *tauABCD* gene cluster (Table 6.10). This decrease in the expression of these genes at 30 min. time point can be correlated with the activation of bacterial defence system.

Table 6.10: Differential expression profile of genes related to cysteine biosynthesis mechanism under the stress of L-Ag NPs.

Gene ID	Gene name	Log_2 fold change		Protein annotation
		5 min.	30 min.	
KPN_RS14865	*cysA*	6.702884	2.027943	Sulfate ABC transporter ATP-binding protein
KPN_RS06815	*cysB*	1.456241	0.62936	LysR family transcriptional regulator CysB
KPN_RS16670	*cysC*	6.730157	1.947889	Adenylyl-sulfate kinase
KPN_RS16680	*cysD*	7.595694	2.981852	Sulfate adenylyltransferase subunit 2
KPN_RS21325	*cysE*	-0.423826	-0.37192	Serine O-acetyltransferase
KPN_RS16685	*cysG*	7.516957	2.806108	Siroheme synthase
KPN_RS16695	*cysH*	4.798077	NSE	Phosphoadenosine phosphosulfate reductase
KPN_RS16705	*cysJ*	4.705464	-0.44536	Sulfite reductase subunit alpha
KPN_RS14815	*cysK*	4.406996	3.026043	Cysteine synthase A
KPN_RS14860	*cysM*	2.365874	1.336362	Cysteine synthase B
KPN_RS16675	*cysN*	7.316089	2.415901	Sulfate adenylyltransferase
KPN_RS14880	*cysP*	5.444071	0.652845	Thiosulfate transporter subunit
KPN_RS24830	*cysQ*	2.402653	2.547014	3'(2')%2C5'-bisphosphate nucleotidase CysQ
KPN_RS02565	*cysS*	0.592421	0.368026	Cysteine--tRNA ligase
KPN_RS14875	*cysU*	6.612925	1.952182	Sulfate/thiosulfate transporter subunit
KPN_RS14870	*cysW*	6.615042	1.739228	Sulfate/thiosulfate transporter permease subunit
KPN_RS14810	*cysZ*	0.633533	1.28024	Sulfate transporter CysZ
KPN_RS01675	*tauA*	5.868925	0.946068	Taurine ABC transporter substrate-binding protein
KPN_RS01680	*tauB*	5.965842	1.581354	Taurine ABC transporter ATP-binding protein
KPN_RS01685	*tauC*	7.406263	1.582485	Taurine ABC transporter permease
KPN_RS01690	*tauD*	5.242747	1.667771	Taurine dioxygenase
KPN_RS05225	*ssuA*	4.076655	1.566315	Aliphatic sulfonate ABC transporter substrate-binding protein
KPN_RS05210	*ssuB*	1.794877	0.99525	Aliphatic sulfonates ABC transporter ATP-binding protein
KPN_RS05215	*ssuC*	2.402878	1.48988	Sulfonate ABC transporter
KPN_RS05220	*ssuD*	4.656351	2.097268	Alkanesulfonate monooxygenase
KPN_RS05230	*ssuE*	5.785325	1.825221	NAD(P)H-dependent FMN reductase

Under the oxidative stress conditions, bacteria also activate its efflux pump machinery to pump out the surplus intracellular silver ions (Gurbanov et al., 2018). As discussed earlier, disturbance in the intracellular protein folding, leads to activate the alternative homeostasis control mechanism, i.e. suf system. Likewise, to remove the surplus silver ions bacteria activates its efflux pump machinery and it is well studied in *E. coli*. In *E. coli*, efflux of heavy inorganic metal like Cu is done by *cusCFBA* regulon, which spans the entire cell envelope. Since Cu and Ag shares the same block and group number in periodic table, *cusCFBA* regulon mechanism can be activated in response to silver also, as discussed in Chapter 4 and 5 (McQuillan et al., 2012). To confirm whether this efflux pump is functional under silver stress or not, we have checked its expression profile and it has been found out that this mechanism for the efflux of silver ions does not apply to *K. pneumoniae* MGH78578 and restricted only to the *E. coli*. Apart from *cusCFBA* regulon, several other genes related to copper efflux system got upregulated in treatment time dependent manner, including *copA, cueO* and two non-annonated genes (KPN_pKPN3p05933 and KPN_RS25550) (Bachman et al., 2015) (Table 6.9).The *cusCFBA* regulon shows homology with the *silCFBA* regulon (silver resistance system) of plasmid pMG101, which belongs to the heavy metal efflux-resistance nodulation division (HME-RND) family of efflux pumps (Gupta et al., 2001; Massani et al., 2018). The transcription of *silCFBA* and *silP* are controlled by the *silRS*, which encodes for a two-component system where SilR acts as a response regulator and SilS acts as a histidine kinase. The SilP is a P-type ATPase efflux pump, which facilitates the passage of silver ion from cytoplasm to the periplasm. SilF protein acts as a chaperone and transfers the silver from periplasm to the SilCBA complex, which is a three-protein dependent cation/proton antiporter system. Another protein from silver resistance system is silE, present downstream to the silRS (Starodub and Trevors, 1989; Massani et al., 2018) (Figure 6.9).

Differential gene expression of silver resistance system shows the expression profile *of silC, silB, silE, silR, silS, silP* and one non-annoted gene KPN_pKPN3p05946. It has been observed that up-regulation in the gene expression is directly proportional to the time of L-Ag NPs exposure (Table 6.11). This up-regulation in the *sil* genes shows the activation of efflux pump machinery as a part of bacterial defence system. Activation of silver resistance system can be linked to the development of resistance against silver ions released from L-Ag NPs. These silver resistant bacterial strains (overexpression of *silP*) can be more toxic due to having probability to transport other traditional antibiotics as well, i.e. generation of antibiotic cross-resistance (Franke, 2007; Randall et al., 2012; Finley et al., 2015; Sütterlin et al., 2017).

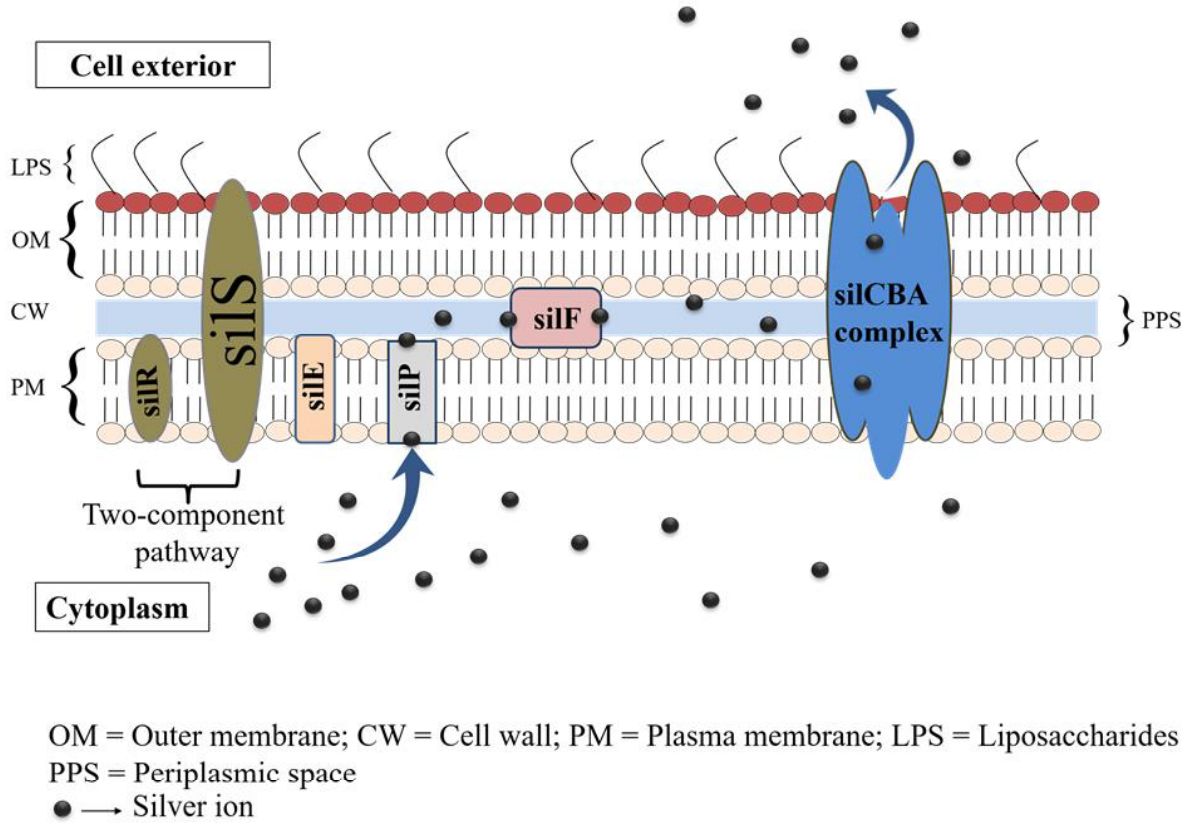

Figure 6.9: Schematic representation of functioning of *sil* system.

Along with *silCFBA* regulon, *K. pnemoniae* also possess AcrAB efflux system. Resistance to numerous categories of antibiotics is related to the overexpression of *acrB* (Okusu et al., 1996; Li and Nikaido, 2009). The AcrAB efflux pump, along with TolC protein is also reported to be involved in the virulence and biofilm formation (Hirakata et al., 2009; Baugh et al., 2013). Differential gene expression profile of these genes found to be up-regulated (~ 2 fold) but not in time-dependent manner. Similarly, another efflux system marABC also plays a peculiar role in the efflux of metals and it is consists of *marA, marB,* and *marC* genes (Anes et al., 2019). Out of three genes, *marA* and *marB* got up-regulated (~ 3 fold) under the stress of L-Ag NPs (Table 6.11).

Table 6.11: Differential expression profile of genes related to efflux pump regulation mechanism under the stress of L-Ag NPs.

Gene ID	Gene name	Log_2 fold change		Protein annotation
		5 min.	30 min.	
KPN_RS02470	*copA*	7.537751	8.276062	Cu^+ exporting ATPase
KPN_pKPN3p05933	KPN_pKPN3p05933	4.91257	8.448544	Probable copper-binding protein
KPN_RS25550	KPN_04739	4.257463	7.33999	Copper transporter
KPN_RS00705	*cueO*	5.618257	6.282559	Multicopper oxidase
KPN_pKPN3p05952	*silE*	4.002173	7.373856	Silver binding protein precursor SilE
KPN_pKPN3p05949	*silC*	5.135199	8.043015	Putative outer membrane protein SilC
KPN_pKPN3p05950	*silR*	2.309241	4.151615	Probable transcriptional regulatory protein (silver resistance)
KPN_pKPN3p05947	*silB*	3.678646	6.891908	Putative membrane fusion protein SilB
KPN_pKPN3p05951	*silS*	1.670652	3.367218	Probable sensor kinase (silver resistance)
KPN_pKPN3p05945	*silP*	0.560048	2.765512	Putative cation transporting P-type ATPase (silver resistance)
KPN_pKPN3p05946	KPN_pKPN3p05946	NSE	4.108267	Exported protein (silver resistance)
KPN_RS02360	*acrA*	2.444486	2.062244	MexE family multidrug efflux RND transporter periplasmic adaptor subunit
KPN_RS02355	*acrB*	1.494705	1.738864	Multidrug efflux RND transporter permease subunit

KPN_RS18470	*tolC*	2.042455	2.765055	Outer membrane channel protein TolC
KPN_RS08735	*marA*	3.670102	3.483579	MDR efflux pump AcrAB transcriptional activator MarA
KPN_RS08730	*marB*	3.616565	3.299014	Multiple antibiotic resistance regulatory periplasmic protein MarB
KPN_RS08750	*marC*	-0.31592	-0.33506	Stress protection protein MarC

As the exposure of L-Ag NPs and removal of silver ions are simultaneous processes, we intended to check that whether the exposure of silver cause the metabolic inactivation of bacteria? To understand this, we performed the differential gene expression analysis of the toxin-antitoxin (TA) system. As discussed in Chapter 4 and 5, it is a set of two or more closely linked genes, which encode a toxin and its corresponding antitoxin protein. This system in basically involved in the stabilization of genome, stress tolerance, phage protection, etc. *K. pneumoniae* used to possess RelBE system, which comes under type II toxin-antitoxin (TA) system. In TA system, toxin and anti-toxin protein interact together and forms a complex to protect the cellular target from the action of toxin (Wei et al., 2016, Fernández-García et al., 2016). Gene expression profiling of the genes related to RelBE system shows either statistically non-significant expression or neutral gene expression, which suggests the metabolically active cell under the treatment of MIC_{75} of L-Ag NPs (Table 6.12).

Table 6.12: Differential expression profile of genes related to toxin-antitoxin system under the stress of L-Ag NPs.

Gene ID	**Gene name**	**Log_2 fold change**		**Protein annotation**
		5 min.	**30 min.**	
KPN_RS21940	KPN_04066	NSE	0.825304	Toxin RelE
KPN_RS25020	relB	NSE	0.504716	Transcriptional regulator

Figure 6.10 represents the heat map of comparative differential expression of genes of all the tested pathways under the exposure of L-Ag NPs for 5 and 30 min. time points.

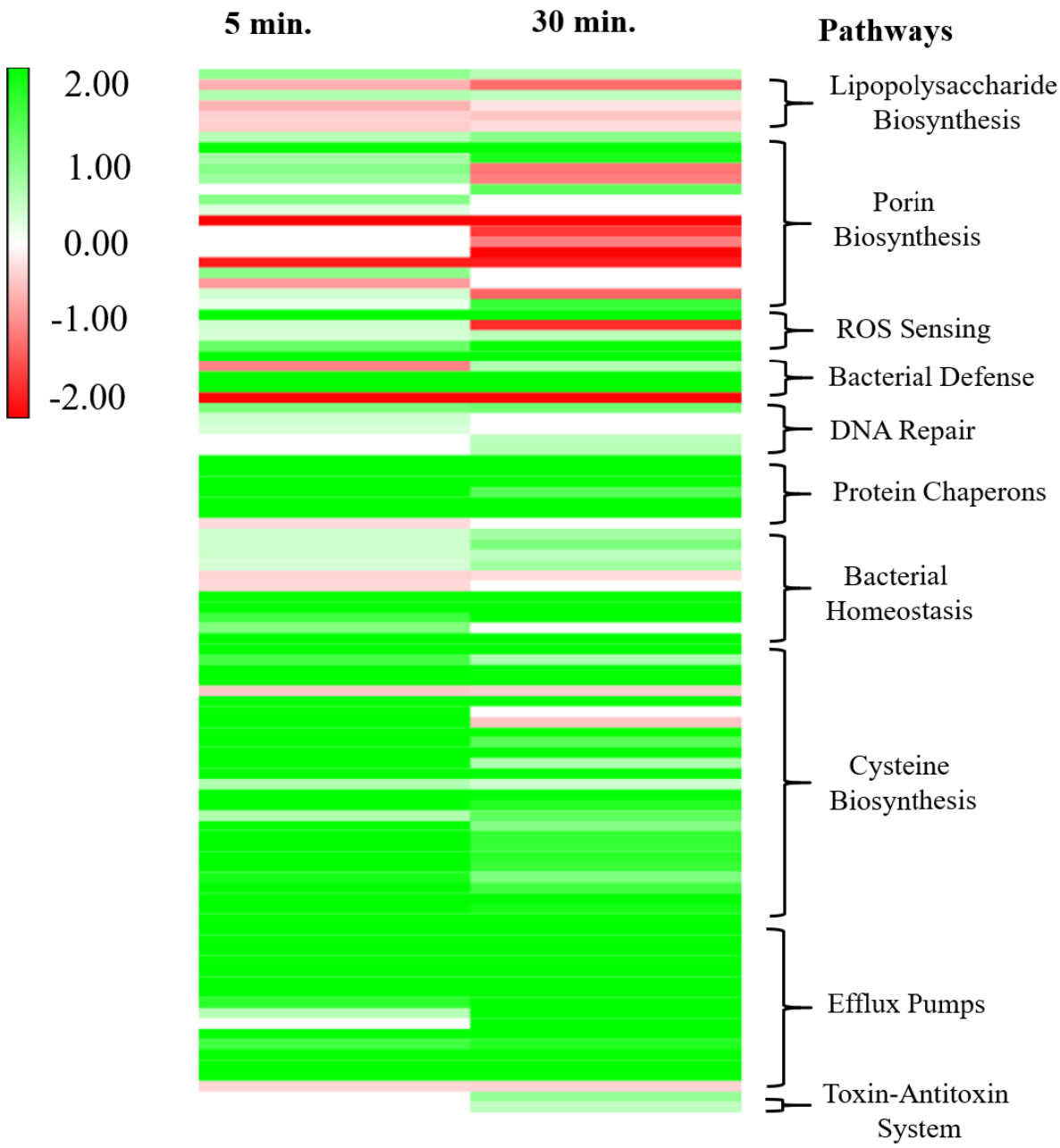

Figure 6.10: Heat map showing expression changes of key genes related to major pathways. The sequence of genes is similar as given in respective table numbers (6.2 to 6.12) (Green and red color denote the up-regulated and down-regulated genes, respectively).

To predict the biological role of genes and their respective functions for the genes, common for 5 and 30 min. treatment, gene ontology (GO) enrichment analysis has been done (Singh et al., 2019) (Figure 6.11).

Biological pathways

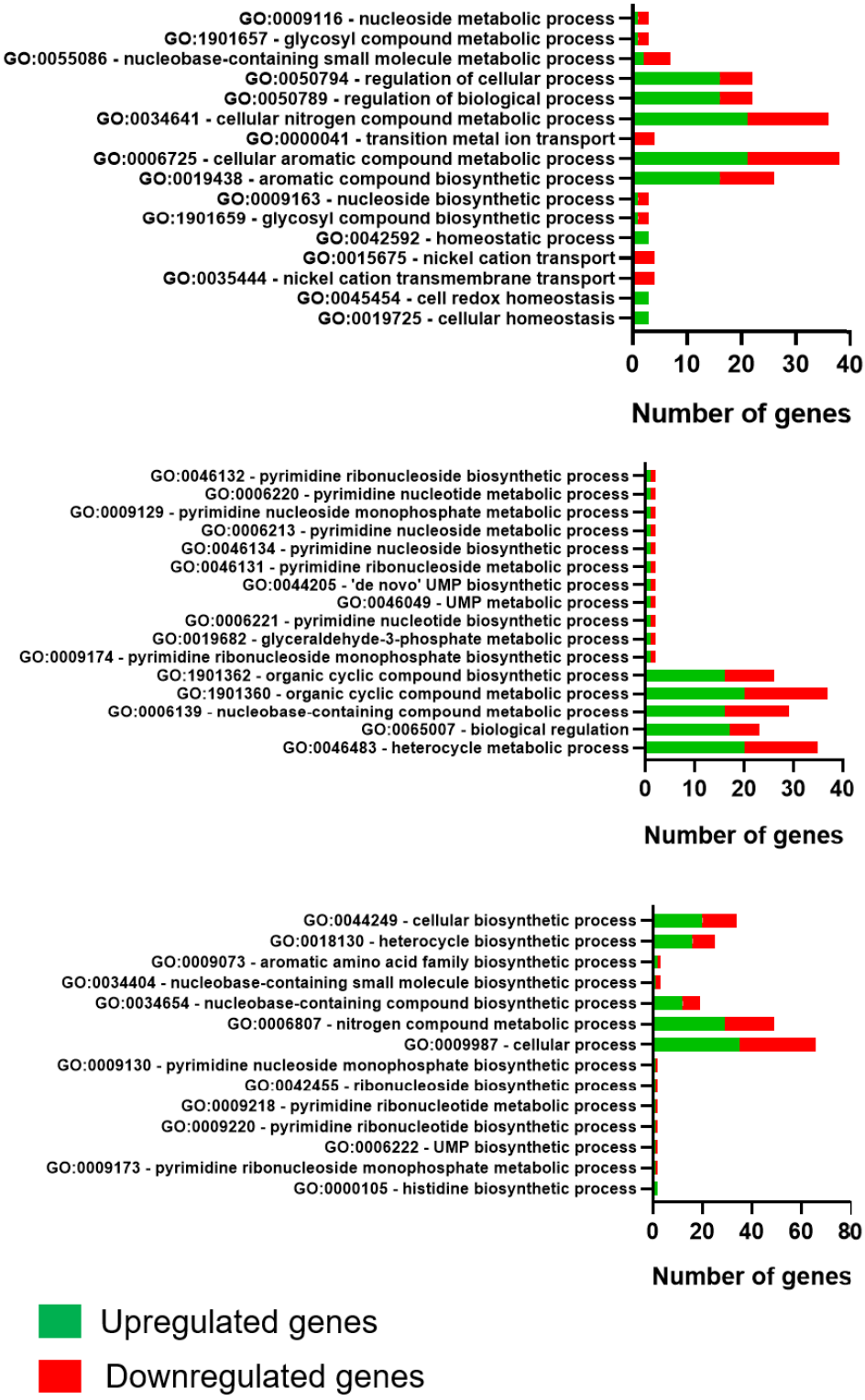

Figure 6.11: GO enrichment analysis of bacterial biological pathways.

GO enrichment analysis showed the involvement of many biological pathways including the cell homeostasis (GO:0019725), redox homeostasis maintenance (GO:0045454), etc. as seen by the individual pathway analysis. Along with Biological pathway, it has also disclosed the commonly expressed (5 min. and 30 min. treatment) cellular components and molecular functions (Figure 6.12).

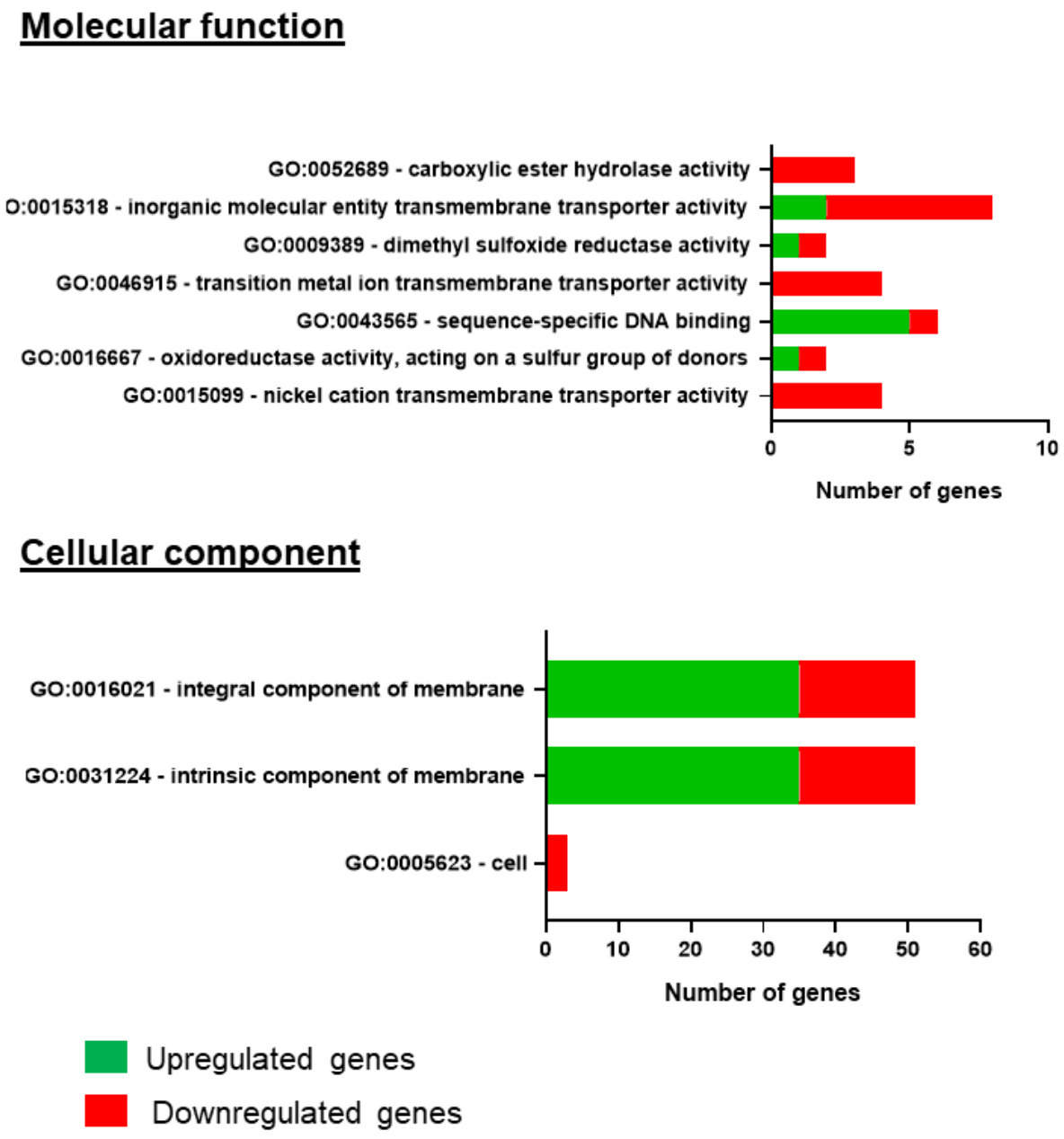

Figure 6.12: GO enrichment analysis of bacterial molecular functions and cellular components.

For the validation of transcriptomic results, qRT-PCR of some of the important genes related to bacterial defence system (*soxS*), transcriptional regulator (*ramA*), outer membrane porin proteins (*ompC*) and virulence (*rfaH*) were done and gene expression was analysed by $2^{-\Delta\Delta Ct}$ method. Gene expression analysis by qRT-PCR reflected the similar results to RNA sequencing data, which further facilitates the strength of RNA seq. based whole transcriptomic analysis.

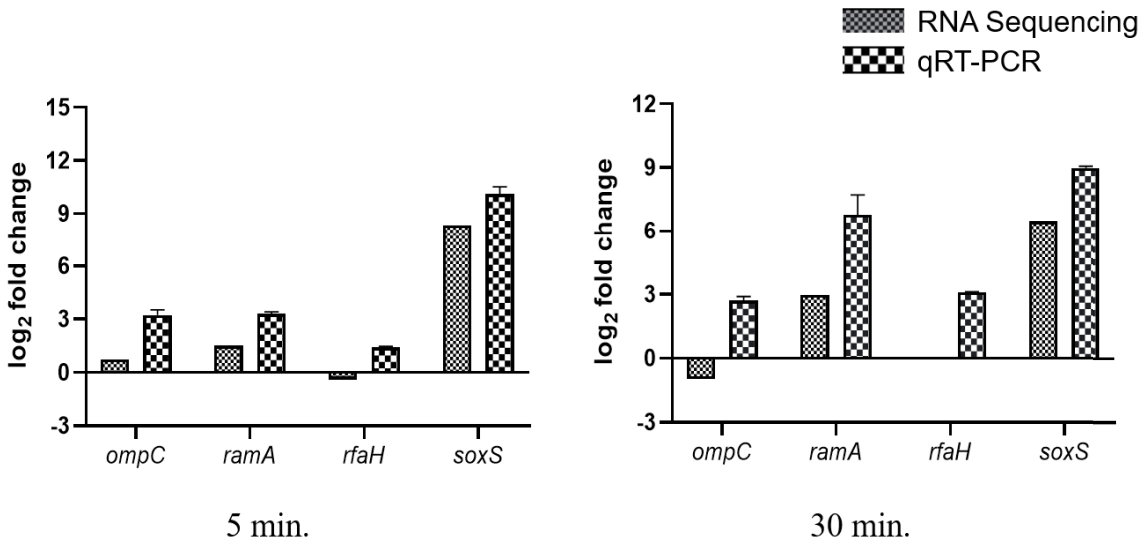

Figure 6.13: Validation measurements comparing the RNAseq and qRT-PCR data at 5 and 30 min, post L-Ag NPs exposure. Vertical bar represents the SD.

6.3.6 Transmission electron microscopy of bacterial cell

Cell integrity and structure damage in the *K. pneumoniae* exposed to MIC_{75} of L-Ag NPs was visualized by TEM imaging. The untreated cells (control) revealed typical rod-shaped structure of *K. pneumoniae* with smooth cell periphery having intact cell wall with no signs of aberration (Figure 6.14 A). No visible changes were observed in the morphology and structure of bacterial cells exposed to L-Ag NPs (Figure 6.14 B). This is the further validation of the results obtained during the biochemical assays of membrane damage analysis, as discussed earlier in this chapter. Multiple spot EDS analysis of bacterial surface showed absence of silver as no characteristic optical absorption band at 3.0 was observed. However, peaks for carbon (1.76 and 0.24 keV), oxygen (0.45 keV) and copper (0.92) were clearly observed, which was due to the use of carbon-coated copper grid for the sample preparation (Figure 6.14 C). The obtained results are in close agreement with the results of biochemical assay and RNAseq analysis.

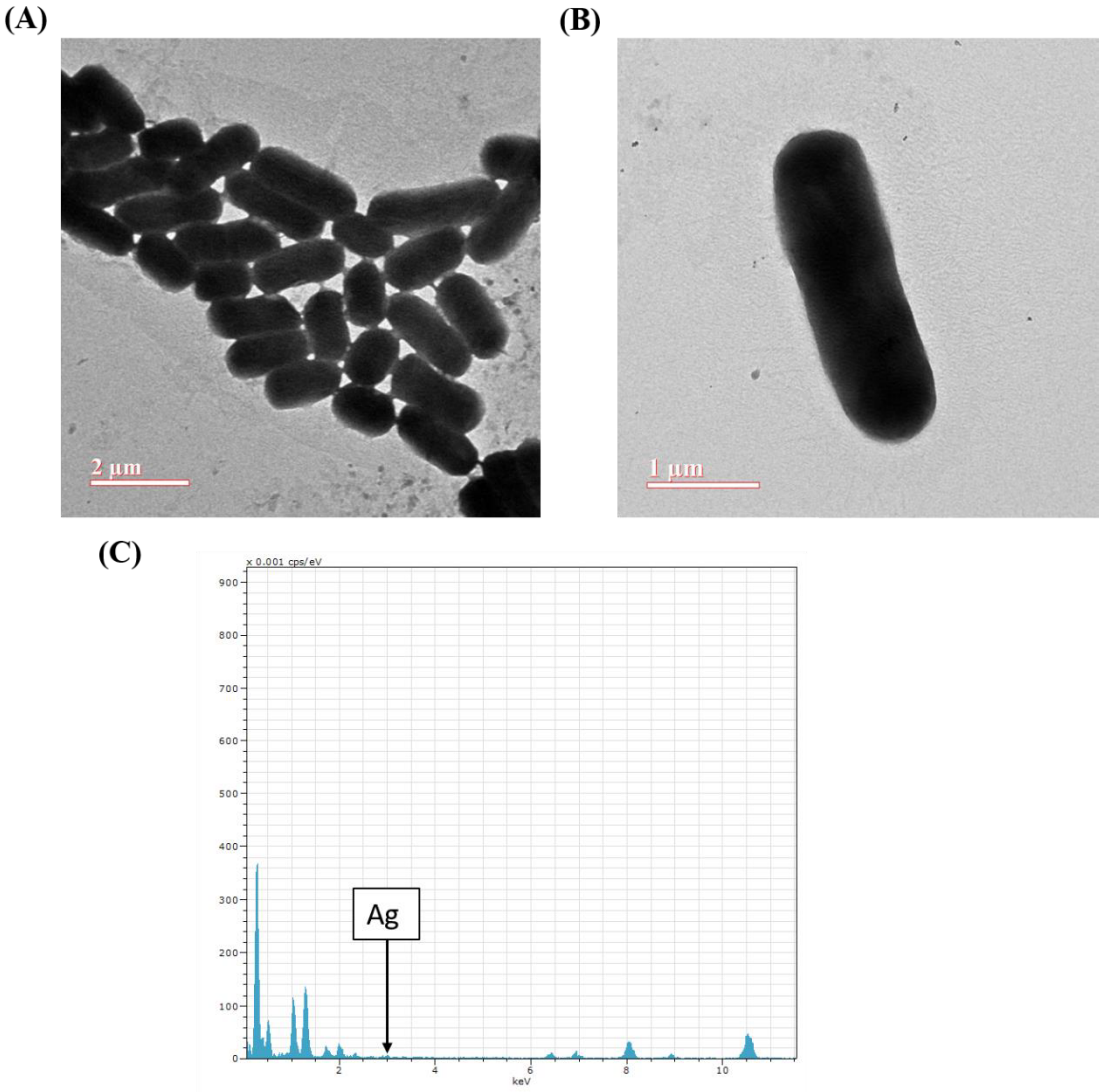

Figure 6.14: TEM micrograph of *K. pneumoniae* MGH78578 exposed to L-Ag NPs (A) control (without exposure), (B) MIC_{75} of L-Ag NPs [6.75 µg (Ag) mL^{-1}], and (C) EDS mapping of bacterial cell surface.

6.4 Conclusion

In the current decade of various antibiotics, Ag NPs are being considered as a potential candidate against multidrug resistant bacterial species including ESKAPE pathogens. To the best of our knowledge, this is the first report where the effect of silver nanoparticles (lysozyme coated) was studied on *Klebsiella pneumoniae* by high throughput transcriptomic profiling, i.e. RNA sequencing.

The current chapter deals with the elucidation of mechanistic aspects behind the antibacterial action of L-Ag NPs against *K. pneumoniae* MGH78578. This has been done by analyzing the antibacterial activity at various stages viz. physiological, biochemical and

molecular levels. Physiological and biochemical analysis has suggested that MIC_{75} has the most impactful impression on antibacterial activity of L-Ag NPs. Hence, molecular studies were done by exposing the *K. pneumoniae* MGH78578 to MIC_{75} of L-Ag NPs for 5 and 30 min., by high throughput technique of RNA sequencing analysis. Transcriptomic profiling of *K. pneumoniae* showed a high number of total reads along with significant ratio of high-quality reads, which confirm the excellent quality and quantity of RNAseq data. As a result, 5357 genes were found to be differentially regulated and 3760 & 3945 genes were found to be statistically significant at 5 min. and 30 min. time points, respectively. To elucidate the complete antibacterial action of L-Ag NPs, various biological pathways have been analysed based on their probable role under the stress of silver species and the obtained RNAseq data were found to be consistent with that of RNAseq analysis of *E. coli* K12, as discussed in Chapter 5.

The neutral behavior of LPS biosynthesis genes and up-regulation of porin protein PhoE, showed the entry of silver ions in the bacterial cell released from L-Ag NPs and confirms the reservoir nature of L-Ag NP. It was observed that both OxyR and SoxRS system functions to sense the silver stress but SoxRS systems shows the predominant activation. Upon the entry of silver in the bacterial cell, ROS was generated in the form of superoxide radicles at the 5 min. time point but at 30 min. time point both superoxide radicles and H_2O_2 contributes towards the generation of ROS. As a defense, *K. pneumoniae* MGH78578 activated the alternate mechanism to maintain the cellular homeostasis i.e. suf system and also activated cysteine biosynthesis machinery. To remove the surplus silver from the bacterial cytoplasm, Cu^+/Ag^+ specific efflux machineries like cue systems was activated along with silver specific system called as Sil system. Activation of silver efflux system (*sil* system) shows the stimulation of bacterial efflux system to throw out the surplus silver from the bacterial cytoplasm. It could also be related to the potential warning for the overuse of silver-based drugs in terms of silver resistance generation. This data further explores the gene pathways and biological processes involved under the exposure of L-Ag NPs. It has suggested that up-regulation of bacterial homeostatic pathways like cellular cation homeostasis, iron ion homeostasis, cellular transition metal ion homeostasis, inorganic ion homeostasis, which helps in the maintenance of bacterial homeostasis under the redox stress conditions. Along with these, pathways related to siderophore metabolic process, enterobactin metabolic process also gets upregulated, which in turn helps in upkeeping the bacterial homeostasis. It has also suggested that biological processes get up-regulated like response to silver ions and redox stress, carbohydrate and polysaccharide biosynthesis process, copper ions homeostasis process, Iron-sulfur cluster

assembly and many more. Overall, this study discloses various options for the generation of target specific silver based antibacterial drugs against *K. pneumoniae* MGH78578. However, considering the use of silver and silver based products as an antibacterial agent in current era of life, further studies need to be done on silver resistance development and the mechanisms involved in it.